Nonadiabatic processes during the oxidation of Li layers

T. Greber, K. Freihube, R. Grobecker, A. Böttcher, K. Hermann, and G. Ertl
Fritz-Haber-Institut der Max-Planck-Gesellschaft, Faradayweg 4-6, D-14195 Berlin, Germany

D. Fick
Philipps-Universität Fachbereich Physik und Wissenschaftliches Zentrum für Materialwissenschaften, D-35032 Marburg, Germany
(Received 7 April 1994)

The first stages of oxidation of thin Li films (leading to the formation of Li_2O) were found to be accompanied by emission of O^- ions as well as electrons, reflecting the participation of electronically highly excited states in this reaction. A model is proposed and supported by the results of local-spin-density-approximation cluster calculations whereby electron transfer from the metal onto the impinging O_2 molecule leads to formation of a transient O_2^{2-} species. This species dissociates without a noticeable activation barrier and there is a finite (but rather low) probability that one of the O^- fragments formed near the surface is ejected into the gas phase. The O^- species at the Li surface forms, on the other hand, a hole state, which subsequently transforms into the O^{2-} ground state. For excitations larger than the work function, the energy associated with its decay (>2 eV) may be released in an Auger process associated with electron emission. The yield of light emission was found to be below the detection limit of about 10^{-10} photons per reacting O_2 molecule and indicates a short lifetime (<100 fs) of the O^- species at a Li surface.

I. INTRODUCTION

Interaction between reactants with strongly differing electronegativities may be associated with transfer of electronic charge as already verified in the gas phase long ago[1(a)] and leading to the famous "harpooning" mechanism.[1(b)] Reactions of this type are not necessarily restricted to the electronic ground state. Nonadiabatic channels may lead to the emission of light or of charge, and their analysis can provide more detailed access to the elementary processes involved. Gas-surface reactions belonging to this category are, for example, offered by the oxidation of alkali metals. Previous studies revealed the emission of exoelectrons, whose intensity with Cs, K, or Na was very small at the initial stages of oxidation and became more pronounced only with the formation of a superoxide.[2-6] For Cs the participation of a surface intermediate was demonstrated to be crucial quite recently.[7] Investigation of the oxidation of Li films, as described in the present paper, was found to be associated with appreciable electron emission already in the early stages of Li_2O formation, where dissociation of the impinging O_2 molecules is involved. It is suggested that this is a consequence of electron transfer and bond-breaking processes in the molecules approaching the surface, which is supported by the parallel observation of ejection of O^- ions [similarly as recently described for the oxidation of Cs (Ref. 8)].

These findings will be corroborated by results of cluster calculations modeling the interaction between O_2 and a Li surface indicating the intermediate formation of O_2^{2-} species, which may dissociate without a noticeable activation barrier. Lastly, a model will be presented that accounts for all experimental and theoretical information available and provides detailed insight into the dynamics of the surface reaction.

II. EXPERIMENT

The experiments were performed in a UHV system (base pressure below 10^{-8} Pa) containing standard facilities for surface preparation and characterization. In particular, information about the electronic properties of the outermost atomic layer could be obtained by means of metastable deexcitation spectroscopy (MDS).[9] The intensities and energy distributions of the negative particles were measured by means of an electrostatic energy analyzer [resolution 500 meV full width at half maximum (FWHM)], which, in addition, provided information about work-function changes. In order to maximize collection of emitted charge the sample was biased on -10 V. The work function Φ was determined from the width ΔE of He I ($h\nu=21.2$ eV) ultraviolet photoelectron spectra (UPS) ($h\nu=\Delta E+\Phi$). Ions ejected from the surface were monitored by a Balzers QMG 421 mass spectrometer. An ion optics collected and focused the ions into the mass spectrometer. From ionic alkali-metal desorption and ion detection in the electrostatic analyzer, the transmission of the instrument was estimated to be between 10^{-3} and 10^{-4}. An additional QMG 112 quadrupole mass spectrometer served for recording thermal-desorption spectra (TDS).

Detection of light emission was attempted by means of a red-sensitive EMI 9130B/350 photomultiplier (PM) ($300<\lambda<800$ nm). In order to improve the signal-to-noise ratio the tube was cooled and operated in a single-photon counting mode with yielding typically 2 counts/s dark current. The PM voltage was set to 1.4 keV yield-

ing maximum signal-to-noise ratio. The photocathode was shielded from stray light through several apertures and mounted in front of a window close to the sample. The photons from 25% of solid angle above the surface were collected and guided in an aluminum mirror tube. The sensitivity of the photocathode to visible light from the sample was checked by the black-body radiation emitted by the sample during its cooling down. This yields typically 10 photons/s at a temperature of 460 K and still 1 photon/s at 430 K.

Lithium was evaporated onto a Ru(0001) substrate from well-outgassed SAES getter sources at typical rates of 0.3 ML per minute. The source was placed in a water-cooled housing with a diaphragm that prevented the alkali atoms from adsorbing on the sample holder. The Li coverage was derived from the thermal-desorption spectra. These have the typical shape reported for alkali overlayers on metals [Fig. 1(a)]: Heating up a sample with a Li concentration exceeding 1 ML produces at first a relatively sharp multilayer peak followed by a broad desorption feature that is attributed to the depletion of the last alkali layer on Ru(0001). As also shown in Fig. 1(a), at very low Li coverages (i.e., at temperatures >1000 K) Li^+ may desorb also, as soon as the work function compares with the ionization potential. Following the Langmuir-Saha equation the splitting ratio between N_i, the number of desorbing positive ions, and N_a, the number of neutrals, is given by a Boltzmann factor $N_i/N_a = 0.5 \exp[(\Phi - I^+)/kT]$, where the prefactor accounts for the degeneracy of the neutral and the ionic Li atoms, respectively. The ionization potential I^+ for Li (5.39 eV) and the work function Φ of clean Ru(0001) (5.37 eV) allows a relatively high ionic desorption rate at low Li coverages, i.e., at high desorption temperatures. This surface ionization effect overcompensates the low ionization probabilities of neutrals in the mass spectrometer and is particularly useful for the study of low alkali-metal coverages on high work-function surfaces. Moreover it is very sensitive to the remaining contamination on the substrate.[10]

Integration of the TDS data from the highest temperature (i.e., zero coverage) continuously down to lower temperatures yields the variation of coverage with T as reproduced in Fig. 1(b). As in other systems [e.g., Cs on Ru(0001) (Ref. 11)] a kink is observed at completion of 1 ML. Thus the intersection point of the two linear extrapolations from the desorption integral from the high coverage (<580 K) and the low coverage (>590 K), respectively, is taken to characterize 1 ML of Li on Ru(0001). This procedure is supported by the results of other experiments, e.g., by low-energy electron diffraction (LEED).[12,13]

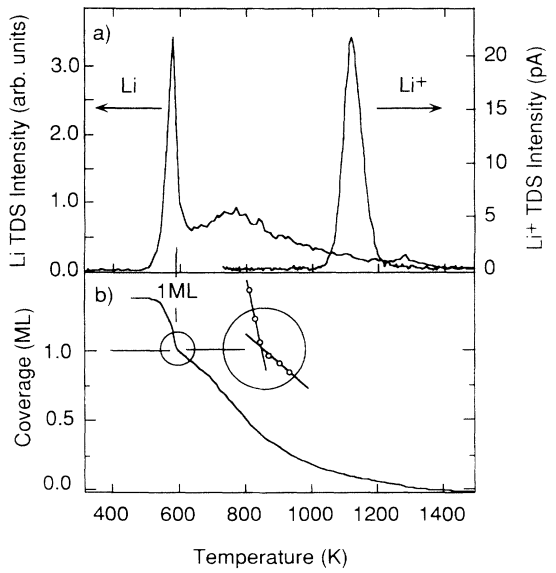

FIG. 1. Thermal desorption (TD) spectra (recorded at a heating rate 6 K/s) of 1.5 ML of Li from Ru(0001). (a) The left scale shows the neutral desorption rate of mass 7 particles, while the sample was kept at -5 V in order to prevent Li^+ from desorption. The right scale shows the positive-ion desorption (0.25 nC of charge is collected in the Faraday cup) that occurs only for large work functions, i.e., low Li coverages. In (b) the coverage as defined in the text is shown.

III. RESULTS

A. Particle emission during oxidation

This section reports the observation of different diabatic fragments ejected from the surface during the oxidation of Li. These fragments are created instantaneously, and thus originate from the oxidation process, getting their energy from the chemical energy released during the reaction.

Figure 2(a) shows the intensity of electrons emitted during the exposure of 2 ML of Li on Ru(0001) as a function of O_2 exposure. The maximum probability corresponds to about $10^{-6} e^-/O_2$. The exoelectron emission starts in the very first oxidation step and decreases before the surface reaches its work-function minimum. The

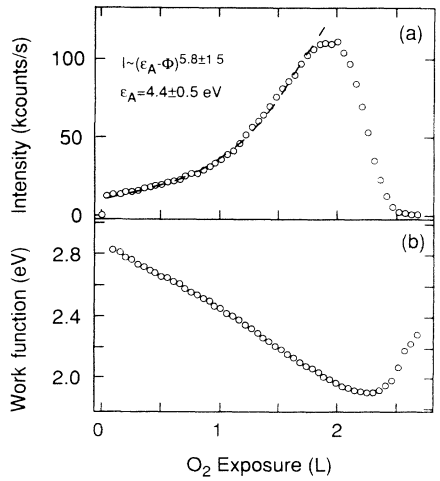

FIG. 2. (a) Yield of exoelectrons form 2-ML Li on Ru(0001) at 300 K exposed to 10^{-6} Pa O_2 as a function of oxygen dose (1 L $= 1.3 \times 10^{-4}$ Pa s). The increase in intensity is fitted to a power law $I \propto (\varepsilon_A - \Phi)^a$. (b) Work function as directly determined from the kinetic-energy distribution of the exoelectrons. The initial value of Φ has been determined from UPS.

work function Φ acts as a high-pass filter for the electrons, i.e., with decreasing Φ the exoelectron intensity increases. The intensity variation with Φ can be approximated by a power law $I \approx (\varepsilon_A - \Phi)^{\alpha}$, where ε_A denotes a maximum excitation energy. The data fit best to an exponent $\alpha = 5.8 \pm 1.5$ and a value of $\varepsilon_A = 4.4 \pm 0.5$ eV [see Fig. 2(a)].

The decrease of the work function of the Li-covered surface ($\Phi_0 = 2.9 \pm 0.1$ eV) with increasing oxygen exposure [Fig. 2(b)] indicates that the oxygen is incorporated beneath the top Li layer because an electronegative particle adsorbed on top of the surface should increase the work function.[14]

Representative energy distributions of exoelectrons at various stages of oxidation are shown in Fig. 3. The resolution of the spectrometer was about 500 meV FWHM. The exoelectron energies are restricted to a narrow range above the corresponding vacuum level and do not exceed a value of about 4.0 eV with respect to the Fermi level. This upper limit is compatible with the value determined from the fit to a power law ($\varepsilon_A = 4.4 \pm 0.5$ eV) as well as with the energy difference calculated for an O^- ion and an O^{2-} ion in a Li cluster (see below).

Figure 4 shows the intensity of exoelectrons as a function of oxygen exposure for various Li coverages analogous to Fig. 2. Obviously emission is strongly coverage dependent. The exoemission process is strongly suppressed in the submonolayer range where the exoemission is smaller than $10^{-10} e^-/O_2$ as compared to 10^{-6} for 2 ML of Li at the exoemission maximum. This cannot be attributed to work-function changes since it does not vary appreciably in the coverage range between 1 and 2 ML where the cutoff is observed.

In further experiments the response of 2-ML Li on NO and CO adsorption were tested. While NO yields similar results to those reported here for O_2, the yield for CO is lower by more than three orders of magnitude. In contrast to NO and O_2, CO has a low probability for dissociation on alkali-metal surfaces so that the chemical energy

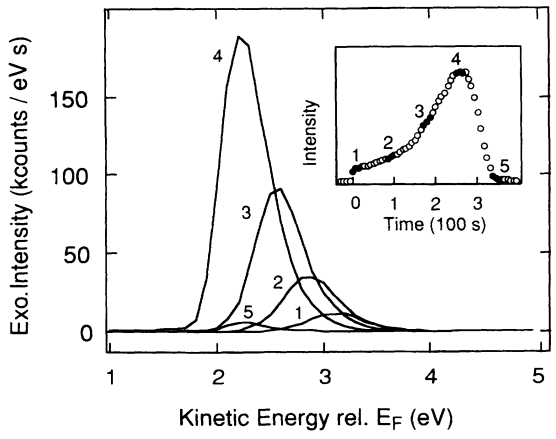

FIG. 3. Kinetic-energy distributions of exoelectrons in five different oxidation stages recorded with an instrumental FWHM resolution of 500 meV. The inset identifies the spectra with the corresponding kinetics. Note the maximum kinetic energy is below 4 eV with respect to the Fermi level.

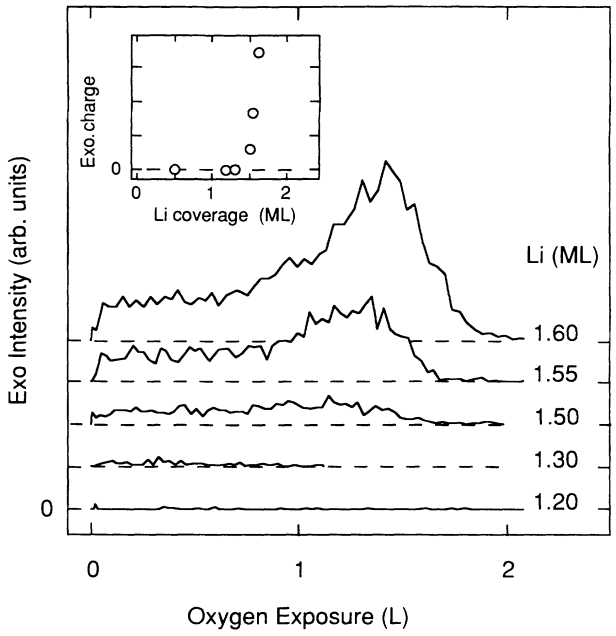

FIG. 4. Exoelectron emission as a function of O_2 exposure for different Li coverages. The intensity recorded for 1.6 ML has two orders of magnitude less intensity than that for 2 ML shown in Fig. 2.

necessary for exoelectron emission is not available.

The emission of light in the course of the reaction is below the detection limit. Figures 5(a) and 5(b) indicate that the number of detected photons for 2-ML Li on Ru(0001) and for a clean Ru(0001) surface exposed to oxygen are of a similar order of magnitude and are in total less than 100 photons from an area of 3×10^{14} Ru atoms. From these values we determine an upper limit for orange (600 nm) light of less than 5×10^{-11} photons/O_2 based on the response function of our PM (6% at 600 nm) and the transmission in our experiment (20%). On the other hand, Fig. 5(c) demonstrates how sensitively the system reacts on Li atoms deposited onto an insulator like the window to the PM. In the calibration procedure, where the sample is heated to 600 K, some Li atoms may adsorb on the window. On further oxygen exposure these atoms emit 1000 photons indicating a chemiluminescence cross section, which is several orders of magnitude larger than that on clean metals.

The low chemiluminescence cross section suggests that the hole for an exoemission process is created very close to the surface, i.e., at a site with high electron density. Here the Auger deexcitation channel leading to exoelectron emission quenches the chemiluminescence channel very effectively.

Parallel to exoelectron emission we find a very faint O^- emission (between 10^{-10} and 10^{-11} O^-/O_2). Figure 6 displays the O^- current detected during O_2 exposure of 2-ML Li on Ru(0001). The O^- current is about two orders of magnitude weaker than that in the $Cs+O_2$ system.[8] This can be rationalized by the larger work function of $Li+O_2$ and, therefore, a much smaller survival probability for an electron in the affinity level of the es-

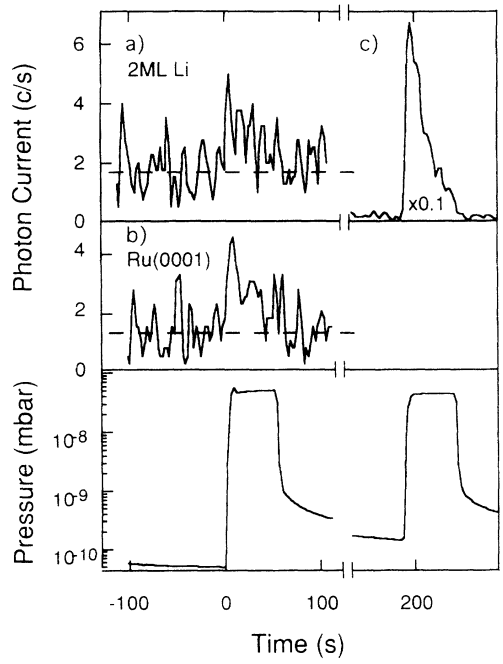

FIG. 5. Photon ($300 < \lambda < 800$ nm) emission during the oxidation of (a) 2 ML of Li on Ru, (b) clean Ru(0001), and (c) from the photomultiplier window with traces of a ML of unoxidized Li adsorbed. The bottom panel shows the corresponding oxygen exposure.

caping oxygen atom (1.46 eV). The crucial role of the work function is again underlined, since the mass 16 current is largest at ~2 L of O_2 exposure where the work function exhibits its minimum (see Figs. 2 and 6). Contrary to the Cs+O_2 system[8] the intensity of emitted O^- does not have its maximum at the beginning of the exposure, which is most likely due to the pronounced influence of the work function in the present system.

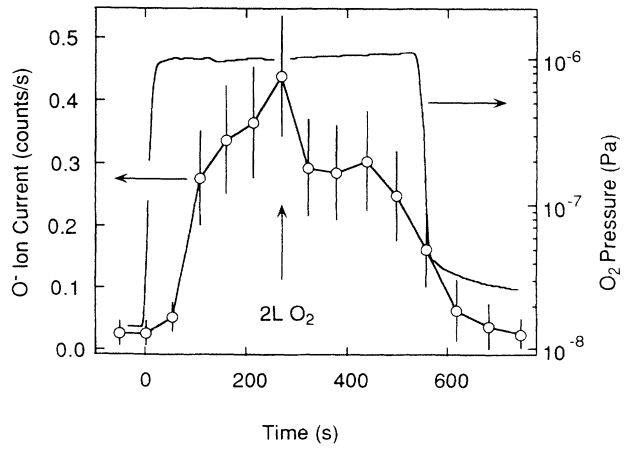

FIG. 6. Detection of negative ions with mass 16 during the oxidation of 2 ML of Li as a function of time. The right-hand scale shows the O_2 pressure exposed to the sample. The maximum ionic emission coincides with the work-function minimum.

B. Electron spectroscopic characterization of the surface

The evolution of the electronic properties of the Li surface was monitored by means of He I ($h\nu = 21.2$ eV) photoemission and metastable 2^1S He (20.6 eV) deexcitation spectroscopy (MDS). The spectra were recorded under a continuous oxygen flux. While photoemission probes several atomic layers, MDS reflects the electronic properties of the outermost atomic layer just as do the impinging gas molecules. MDS is therefore a particularly well-suited tool to correlate the electronic situation felt by the incident molecules that eventually gives rise to emission of exoelectrons.

Figure 7 compares UPS and MDS with exoemission (Fig. 2), from 2-ML Li on Ru(0001), as a function of oxygen dose. Conversion of the kinetic energies into a binding-energy scale is straightforward for UPS because the excitation energy is fixed. This is not the case for the MDS data. That is why there the experimental kinetic-energy scale is chosen and the position of the Fermi energy is indicated with a spread of about 1 eV [Fig. 7(b)].

The UPS show the presence of occupied states up to the Fermi level over the whole range of exposure. The peaks at 2.4- and 4.9-eV binding energy are Ru 4*d*-band features.[15] With increasing O_2 exposure a single peak grows at ~5.2-eV binding energy, which is attributed to O 2*p*-derived states. Its appearance is closely connected to the formation of Li_2O.[16,17] After the work-function

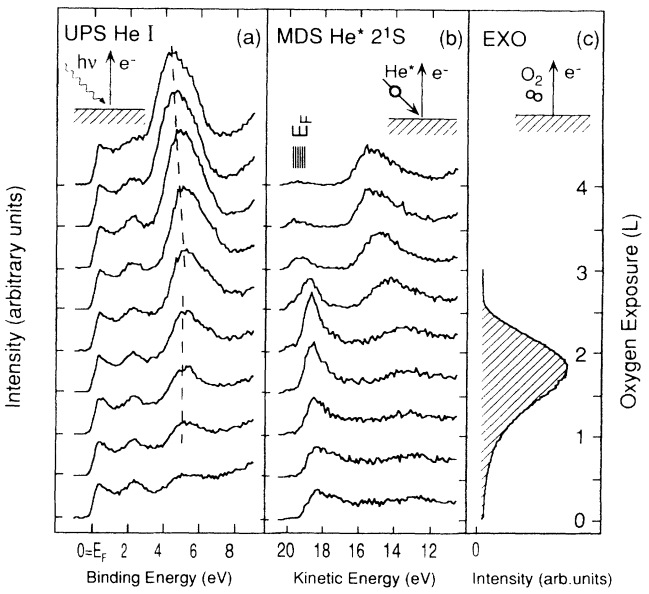

FIG. 7. Spectroscopic investigations of the oxidation of about 2 ML of Li on Ru(0001). In (a) UPS are shown that still reflect some emission from the Ru 4*d* band and that show an oxide peak to grow at 5.2-eV energy that shifts towards lower binding energy after the work-function minimum. In (b) complementary MDS are shown, which indicate that the gas-surface interface remains metallic down to the work-function minimum, after which an oxygen 2*p*-related feature is growing. In (c) the exoelectron emission yield is shown as a function of oxygen exposure.

minimum at ~2 L of O_2 exposure this oxygen feature shifts to lower binding energy (4.4 eV). This may indicate that in this stage, where exoelectron emission no longer occurs, higher oxides are formed.

The MDS in Fig. 7(b) show a pronounced contribution from states near the Fermi level until the work-function minimum is reached. This indicates that the gas-solid interface remains metallic in this range. Their intensity decays rapidly parallel to the decrease of exoelectron emission. Simultaneously another spectral feature emerges at lower kinetic energies and shifts continuously relative to E_F, analogous to the UPS data. Obviously oxygen is no longer incorporated below the surface but also "sticks" into the vacuum.

The spectroscopic data reflect the formation O^{2-} ions and thus of Li_2O in the first oxidation step. The MDS indicate that the ions incorporate beneath the top Li layer since the oxygen feature around a kinetic energy of 15 eV appears only after the exoelectron emission drops. This latter conclusion is supported by the work-function decrease, which is attributed to the formation of subsurface oxygen. All these findings are consistent with a recent MDS-UPS study for the oxidation of Li on a W(110) surface, for which it was found that beyond 1.4 ML of Li O^{2-} ions are no longer formed.[17]

C. Cluster-model calculations

In order to obtain closer insight into the dynamics of the elementary steps leading to the emission of exoelectrons and O^- ions, cluster calculations were performed. The theoretical approach is based on density-functional theory using the local-spin-density approximation (LSDA). Total energies of Li_nO_m ($n=8,10,14$, $m=1,2$) were obtained as a function of the oxygen coordinates (distance and orientation) relative to the Li substrate. The Li_n cluster mimics an ideal bcc (100) surface with lattice constant $a_0=3.45$ Å. The lateral reaction coordinate was chosen for the oxygen approach at a bridge site, which was found most favorable in an early Hartree-Fock cluster study.[18,19] Further technical details are described elsewhere.[20] The LSDA calculations yield potential hypersurfaces for the cluster ground state and selected excited states (determined as ground states with spin and symmetry constraints), which together with the character of the electronic configuration can give information about possible reaction paths in the adiabatic approximation. While these calculations cannot describe the detailed dynamics of the oxidation process they assist in identifying important reaction steps.

As an example of the calculations, contour plots of Figs. 8(a) and 8(b) show scaled total-energy hypersur-

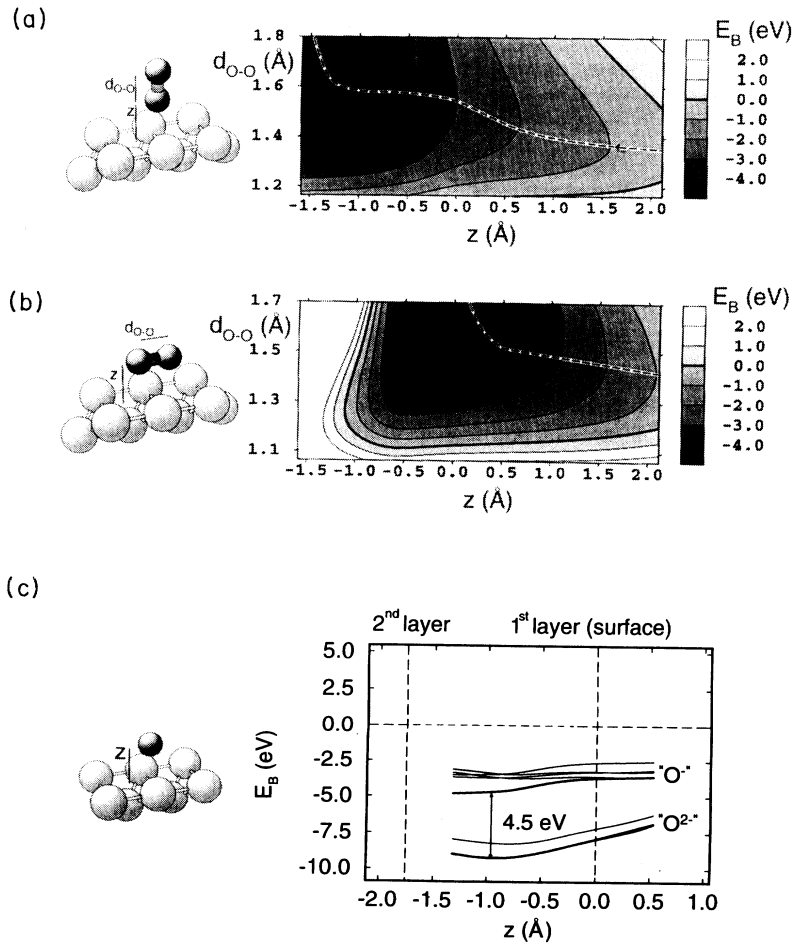

FIG. 8. Results from the total-energy LSDA calculations on an O_nLi_m cluster as a function of the O coordinates d and z relative to the central-bridge site of the top Li layer. (a) The O_2 molecule approaches the surface in normal geometry. From the parallel contours for $h<0$ it is seen that even for this unfavorable geometry the O_2 bond is lifted as soon as the first oxygen penetrates into the surface. O_2 will dissociate into two O^- ions (b) as (a) with parallel O_2 approach. In (c) ground-state O^{2-} and restricted ground-state O^- calculations are shown. The deexcitation energy from $O^- \rightarrow O^{2-}$ is found to be 4.5 eV.

faces of the $Li_{10}(6,4)O_2$ cluster for O_2 approaching at the Li bridge site with the molecular axis pointing perpendicular [Fig. 8(a)] and parallel [Fig. 8(b)] to the surface. The coordinates of the plots are the normal position z of the molecule with respect to the first Li layer and the intramolecular distance $d_{O\text{-}O}$. Figures 8(a) and 8(b) clearly show that in both adsorption geometries the O_2 molecule is attracted quite strongly by the Li substrate, where it can get near the surface and may even penetrate partially below the first layer [$z=0$, perpendicular approach, Fig. 8(a)]. In addition, the $d_{O\text{-}O}$ dependence of the cluster total energy becomes rather weak near the surface indicating a strongly reduced strength of the O-O bond, which allows dissociation of the adsorbed molecule without any noticeable activation barrier. The origin of the dramatic O-O bond weakening becomes evident from cluster-orbital analyses.[21] As a result of O_2 interacting with the Li substrate there is a charge transfer from the metal to the molecule leading, in the cluster ground state, to an effective O_2^{2-} species near the surface. The additional adsorbate charge is about evenly distributed between the oxygen atoms and is combined with a filling of O_2 $1\pi_g$-type orbitals. Since the O_2 $1\pi_g$ orbitals are antibonding within the molecule the charge transfer near the surface weakens the O-O bond.

The O^- species formed in front of the surface after O_2 dissociation does not, however, represent the electronic ground state. This becomes evident from inspection of Fig. 8(c), which depicts the potential of the ground state and of several excited state of the $Li_8(6,2)O$ cluster as a function of the oxygen coordinate z perpendicular to the surface, where $z=0$ denotes the first Li layer and the oxygen is placed at the bridge site. The energetically lowest curve denoting the cluster ground state shows that the adsorbed oxygen is bound quite strongly and stabilizes below the first Li layer ($z<0$). A Mullikan charge analysis reveals an ionic O^{2-} species, analogous to the situation in lithium oxide, Li_2O. There are, however, excited states at 4–5 eV above the ground state, see Fig. 9(c), where the oxygen is bound below the Li surface and is characterized as O^- from charge and spin analysis. These results suggest that the O^- species produced by the O_2 dissociation near the surface will eventually undergo a deexcitation into O^{2-}, which process is predicted to be associated with an energy release of the order of 4–5 eV.

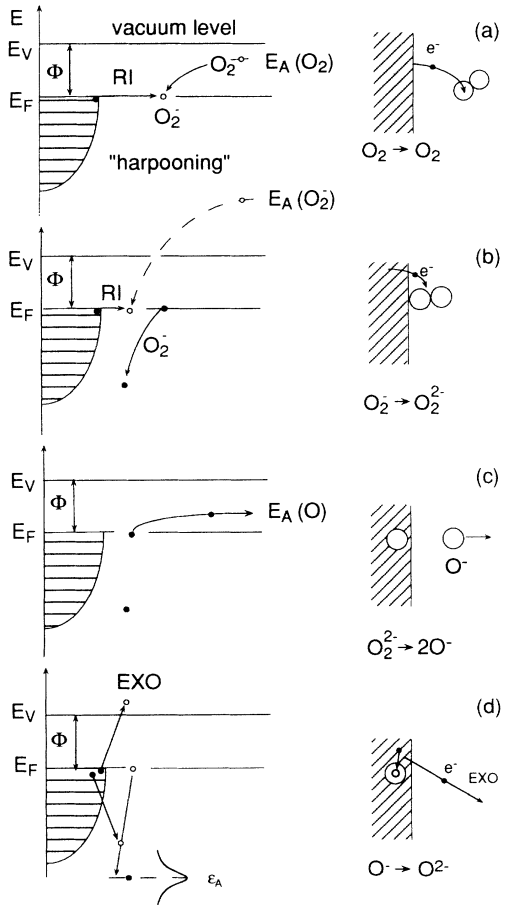

FIG. 9. Model for the oxidation of Li leading to the observed nonadiabatic particles. On the left-hand side a one-electron picture and on the right-hand side the corresponding geometric situation is shown. (a) The O_2 molecule approaches the surface and becomes harpooned by a substrate electron. The O_2^- ion accelerates toward the surface and (b) may form an O_2^{2-} intermediate that dissociates into two O^- ions. For normal geometry (c) one O^- ion may escape the surface. The deexcitation of the remaining O^- ions into the O^{2-} ground state may proceed via the emission of an exoelectron into the vacuum (d).

IV. DISCUSSION

The chemical energy provided by the oxidation of Li may in part be released via nonadiabatic channels as manifested by the observation of electron and O^- emission. In the following the discussion will concentrate on the early stages of oxidation where O_2 interacts with the bare Li surface and eventually leads to the formation of Li_2O units.

Figure 9 sketches schematically in a one-electron picture the various processes involved as follows.

(a) The affinity level of an incident O_2 molecule becomes continuously lowered due to image force and chemical interaction until it crosses the Fermi level, where the "harpooning" effect causes resonance ionization into O_2^-.

(b) The O_2^- species is accelerated towards the surface and will at even shorter distance pick up a second electron. This step corresponds to the transition of O_2^- to O_2^{2-}. From the theoretical total-energy hypersurfaces of Figs. 8(a) and 8(b) it becomes evident that the O_2^{2-} will readily dissociate into two O^-'s, regardless of the geometry of the molecular axis. This accounts for the observed very high reaction probability.

(c) The two O^- fragments resulting from the bursting O_2^{2-} species will, in most cases, both be strongly attracted by the surface and decay into the ground state. For special configurations such as depicted schematically in Fig. 9(c), however, there will be a finite, albeit small,

probability that one of the O^- ions will be ejected into the vacuum. (It should be noted here that O^- was the only ionic species that could be detected by mass spectrometry.)

(d) The O^- species will not represent the stable ground state of an oxygen atom interacting with a Li surface. Oxygen will rather become an O^{2-} ion, which according to the calculations [Fig. 8(c)] will be energetically favorable by about 4.5 eV. In a one-electron picture the affinity level of O^- will be degenerate with E_F during the moment of its creation and will subsequently start to "dive" towards it final energy ε_A, which equals the binding energy of the O 2*p*-derived peak in UPS and MDS at about 5 eV below E_F.

If this hole on the excited O^- ion would suddenly be created at ε_A, its decay via Auger deexcitation[22] [Fig. 9(d)] would give rise to exoelectrons with maximum kinetic energy (if both electrons involved originate from the Fermi level) of $\varepsilon_A \approx 5$ eV. Inspection of Fig. 3 demonstrates that the actual kinetic energies are lower by more than 1 eV. This is (at least in part) due to the fact that the hole at the O^- ion has a finite lifetime τ, which competes with the time scale t of the nuclear motion.

If the hole would suddenly be created at ε_A, inspection of Fig. 9(d) shows that the yield of exoelectrons would be governed by the difference $(\varepsilon_A - \Phi)$; that means the work function acts as a high-pass filter. Within a simplified model the intensity of exoelectron emission is predicted to vary with the work function Φ according to a power law $\propto (\varepsilon_A - \Phi)^{5/2}$.[22] (An earlier study arrived at a cubic law[23] where the difference is due to different expansions in solving the convolution integral between the intrinsic Auger electron-energy distribution and the escape function.) The exponent 2.5 is at variance with the best fit of 5.8 ± 1.5 to the experimental data of Fig. 2. This has in part to be attributed to the progressing oxidation, which continuously reduces the fraction of the surface that is exoactive. But even if an exponential decrease of this fraction with exposure is taken into account, the resulting exponent would still be outside the experimental value of 5.8 ± 1.5.

If, however, the hole after its creation has a finite decay probability already on its way down to ε_A, a larger exponent can readily be rationalized. A model for "hole diving" taking into account these effects has been developed elsewhere.[22] It contains three steps, namely, electronic excitation by chemical reaction, subsequent Auger deexcitation, and refraction of the electrons created inside the solid at the potential arising from the work function. The experimentally observed exoelectron yields are adequately described by reaction times t which are about 50–100 times the O 2*p* lifetime τ at ε_A. From the kinetic-energy distribution of the exoelectrons τ is estimated to be about 10^{-15} s. Consequently the reaction times during which the O_2^{2-} species fall apart are estimated to be of the order 10^{-13} s, which is in the range of molecular-vibration periods.

The model described here is based on the recently proposed mechanism for the emission of O^- ions in the first oxidation stage of Cs.[8] But in contrast to the oxidation of Cs for Li, a high-electron emission probability is observed in the first oxidation stage. This may be rationalized by the much smaller bandwidth of Cs (1.6 eV) as compared to 4.6 eV for Li, since the ratio between the heat of formation for the alkali oxides (A_2O) and the corresponding work functions increase linearly with the bandwidth. Apparently the bandwidth-to-work-function ratio of Cs is not large enough for a considerable production of exoelectrons. In recent work it is shown that the exoelectron emission probability drops considerably if the work function increases relative to the final affinity ε_A.[22] In the case of Cs and Na, however, appreciable exoelectron emission is observed at a late stage of the oxidation.[3–7] It could recently be demonstrated that with partly oxidized Cs the emission of exoelectrons proceeds via thermally stimulated dissociation of an O_2^- species on top of the surface and the subsequent incorporation of the fragments beneath the Cs.[7] In this case the exoemission process may again be related with the transfer of the second electron on an O^- ion after breaking of the molecular bond.

The effects of exoelectron emission associated with the interaction of Cs with different nitric oxides, i.e., NO, NO_2,[24] and N_2O,[25] are also compatible with the proposed model. For NO_2 (2.2 eV) and for N_2O (1.4 eV) (the values in parentheses are the electron affinities of the free molecules with respect to the vacuum level) it is found that exocelectrons are emitted at the beginning of the dissociative adsorption. The difference between exoelectron emission for O_2 and NO on the one hand and NO_2 and N_2O on the other can be qualitatively attributed to the higher electron affinities of the latter molecules. These higher affinities cause the first electron transfer from the solid to the molecule to happen further away from the surface and therefore allow the negative ion to pick up more kinetic energy, which will increase the probability for nonadiabatic events.

The proposed model is in accordance with previous concepts presented by Nørskov, Newns, and Lundqvist[26] and Kasemo *et al.*[27] It labels and quantifies the electronic states on which the excitation occurs and it incorporates, as well, ionic emission as a possible nonadiabatic channel. It can be concluded that for the oxidation of alkali-metal surfaces, the exoactive deexcitation step must happen closer to the surface than that in the case of Cl_2 on Na and K.[28] This is due to the fact that the affinity levels of Cl_2 (2.38 eV) and O_2 (0.44 eV) differ considerably and that, therefore, for Cl_2 the first charge transfer occurs further away from the surface than with O_2. Furthermore, in the first oxidation step there are two electrons transferred on the oxygen atom, where there is only one electron transferred to a Cl atom.

In conclusion, the observation of nonadiabatic reaction products as electrons and O^- ions during the reaction of O_2 with Li metal is reported. Together with LSDA calculations and spectroscopic investigations a dynamic model for this reaction is drawn. The O^- ions are fragments from the O_2 dissociation that is shown to proceed via O_2^{2-} formation. The exoelectrons, on the other hand, stem from an Auger transition of the intermediate O^- species into the O^{2-} ground state.

ACKNOWLEDGMENTS

For T.G. it is a pleasure to acknowledge financial support from the Schweizerischen Nationalfonds and the Alexander von Humboldt Stiftung. D.F. appreciated the warm hospitality of the Fritz-Haber-Institut for several months during which part of this work was done. The work was supported in part by Deutsche Forschungsgemeinschaft (Sonderforschungsbereich 290, Berlin).

[1](a) H. Beutler and M. Polany, Z. Phys. **47**, 379 (1928); (b) D. R. Herschbach, Adv. Chem. Phys. **10**, 319 (1966); R. D. Levine and R. B. Bernstein, *Molecular Collision Theory* (Clarendon, Oxford, 1974).

[2]B. Kasemo and L. Walldén, Surf. Sci. **75**, L379 (1978).

[3]A. Böttcher, R. Imbeck, A. Morgante, and G. Ertl, Phys. Rev. Lett. **65**, 2035 (1990).

[4]A. Böttcher, R. Grobecker, R. Imbeck, A. Morgante, and G. Ertl, J. Chem. Phys. **95**, 3756 (1991), and references therein to earlier literature.

[5]H. Brenten, H. Müller, W. Maus-Friedrichs, S. Dieckhoff, and V. Kempter, Surf. Sci. **206**, 151 (1992).

[6]A. Böttcher, R. Grobecker, T. Greber, A. Morgante, and G. Ertl, Surf. Sci. **280**, 170 (1992).

[7]R. Grobecker, H. Shi, H. Bludau, T. Hertel, T. Greber, A. Böttcher, K. Jacobi, and G. Ertl, Phys. Rev. Lett. **72**, 578 (1994).

[8]T. Greber, R. Grobecker, A. Morgante, A Böttcher, and G. Ertl, Phys. Rev. Lett. **70**, 1331 (1993).

[9]J. Lee, C. Hanrahn, J. Arias, F. Boszo, R. M. Martin, and H. Metiu, Phys. Rev. Lett. **54**, 1440 (1985); B. Woratschek, W. Sesselmann, J. Küppers, G. Ertl, and H. Haberland, *ibid.* **55**, 611 (1985); A. Böttcher, A. Morgante, R. Grobecker, T. Greber, and G. Ertl, Phys. Rev. B **49**, 10 607 (1994).

[10]T. Greber, A. Morgante, R. Grobecker, A. Böttcher, and G. Ertl (unpublished).

[11]H. Over, H. Bludau, M. Skottke-Klein, G. Ertl, W. Moritz, and C. T. Campbell, Phys. Rev. B **45**, 8659 (1992).

[12]D. L. Doering and S. Semancik, Surf. Sci. **175**, L730 (1986).

[13]H. Bludau and M. Gierer (private communication). In their LEED study the absolute Li coverage of 1 ML Li on Ru was determined to $\theta=0.75\pm0.1$ corresponding to 1.2×10^{15} Li atoms/cm^2. This value is at some variance to that in Ref. 12 ($\theta=0.46$).

[14]B. Woratschek, G. Ertl, J. Küppers, W. Sesselmann, and H. Haberland, Phys. Rev. Lett. **57**, 1484 (1986); J. Hölzl, F. K. Schulze, and H. Wagner, *Work Function of Metals,* edited by G. Hohler and E. A. Niekisch, Springer Tracts in Modern Physics Vol. 85 (Springer, Berlin, 1979).

[15]F. J. Himpsel, K. Christmann, P. Heimann, and D. E. Eastman, Phys. Rev. B **23**, 2548 (1981).

[16]J. Jupille, P. Dolle, and M. Besançon, Surf. Sci. **260**, 271 (1992).

[17]W. Maus-Friedrichs, S. Dieckhoff, M. Wehrhahn, S. Plüm, and V. Kempter, Surf. Sci. **271**, 113 (1992).

[18]K. Hermann, in *Proceedings of the Seventh International Vacuum Congress and the Third International Conference on Solid Surfaces, Vienna, 1977,* edited by R. Dobrozemsky *et al.* (F. Berger & Sohne, Vienna, 1977), Vo. II, p. 943.

[19]K. Hermann and P. S. Bagus, Phys. Rev. B **17**, 4082 (1978).

[20]K. Freihube, Ph. D. thesis, Free University, Berlin, 1993; K. Freihube and K. Hermann (unpublished).

[21]K. Hermann, K. Freihube, T. Greber, A. Böttcher, R. Grobecker, D. Fick, and G. Ertl, Surf. Sci. **313**, L806, (1994).

[22]T. Greber, Chem. Phys. Lett. **222**, 212 (1994).

[23]R. H. Prince, R. Lambert, and J. S. Foord, Surf. Sci. **107**, 605 (1981).

[24]A. Böttcher, R. Grobecker, T. Greber, and G. Ertl, Chem. Phys. Lett. **208**, 404 (1993).

[25]T. Gießel, A Böttcher, T. Greber, and G. Ertl (unpublished).

[26]J. K. Nørskov, D. M. Newns, and B. I. Lundqvist, Surf. Sci. **80**, 179 (1979).

[27]B. Kasemo, E. Törnqvist, J. K. Nørskov, and B. I. Lundqvist, Surf. Sci. **89**, 554 (1979).

[28]D. Andersson, B. Kasemo, and L. Walldén, Surf. Sci. **152/153**, 576 (1985).

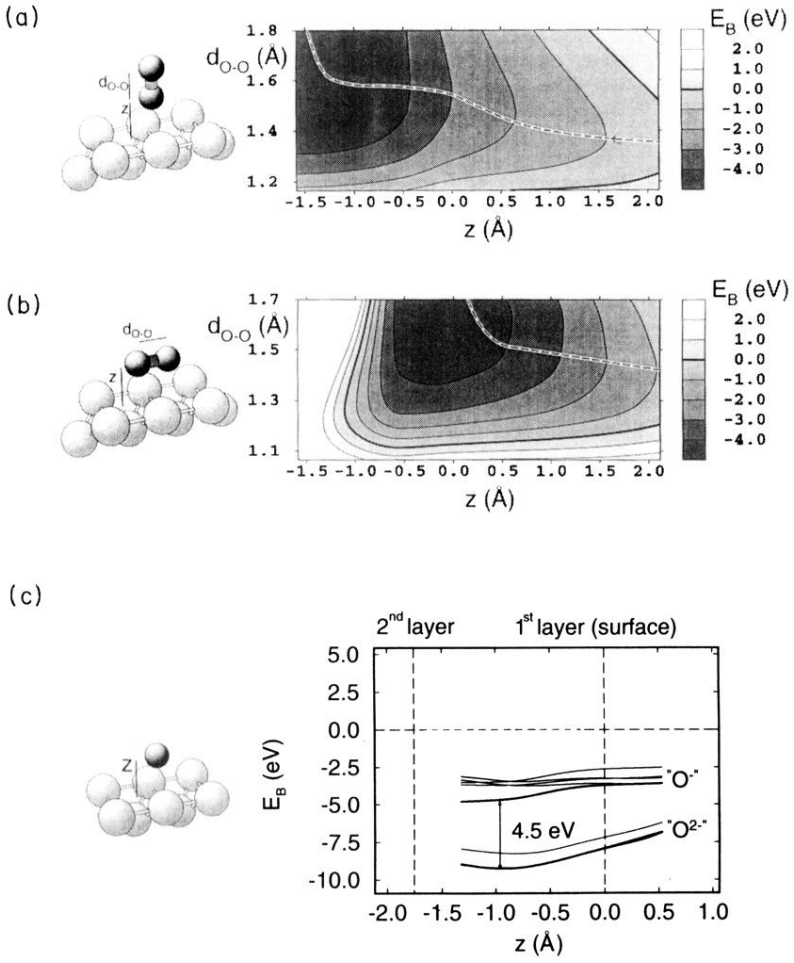

FIG. 8. Results from the total-energy LSDA calculations on an O_nLi_m cluster as a function of the O coordinates d and z relative to the central-bridge site of the top Li layer. (a) The O_2 molecule approaches the surface in normal geometry. From the parallel contours for $h<0$ it is seen that even for this unfavorable geometry the O_2 bond is lifted as soon as the first oxygen penetrates into the surface. O_2 will dissociate into two O^- ions (b) as (a) with parallel O_2 approach. In (c) ground-state O^{2-} and restricted ground-state O^- calculations are shown. The deexcitation energy from $O^-\rightarrow O^{2-}$ is found to be 4.5 eV.